BULLETIN OF THE POLISH ACADEMY OF SCIENCES
TECHNICAL SCIENCES, Vol. 64, No. 3, 2016
DOI: 10.1515/bpasts-2016-0059

Si/ZnO nanorods with Ag nanoparticles/AZO heterostructures in PV applications

K. GWÓŹDŹ*[1], E. PŁACZEK-POPKO[1], Z. GUMIENNY[1], E. ZIELONY[1], R. PIETRUSZKA[2], B. S. WITKOWSKI[2], Ł. WACHNICKI[2], S. GIERAŁTOWSKA[2], M. GODLEWSKI[2,3], and L. B. CHANG[4]

[1]Department of Quantum Technologies, Faculty of Fundamental Problems of Technology, Wroclaw University of Science and Technology, 27 Wybrzeze Wyspianskiego, 50-370 Wroclaw, Poland

[2]Institute of Physics, Polish Academy of Sciences, 32/46 Lotnikow Av., 02-668 Warsaw, Poland

[3]Department of Mathematics and Natural Sciences College of Science, Cardinal Stefan Wyszynski University, 5 Dewajtis St., 01-815 Warsaw, Poland

[4]Department of Electronic Engineering and Green Technology Research Center, Chang-Gung University, Taoyuan, Taiwan

Abstract. Our studies focus on test structures for photovoltaic applications based on zinc oxide nanorods grown using a low-temperature hydrothermal method on a p-type silicon substrate. The nanorods were covered with silver nanoparticles of two diameters – 20–30 nm and 50–60 nm – using a sputtering method. Scanning electron microscopy (SEM) micrographs showed that the deposited nanoparticles had the same diameters. The densities of the nanorods were obtained by means of atomic force microscope (AFM) images. SEM images and Raman spectroscopy confirmed the hexagonal wurtzite structure of the nanorods. Photoluminescence measurements proved the good quality of the samples. Afterwards an atomic layer deposition (ALD) method was used to grow ZnO:Al (AZO) layer on top of the nanorods as a transparent electrode and ohmic Au contacts were deposited onto the silicon substrate. For the solar cells prepared in that manner the current-voltage (I-V) characteristics before and after the illumination were measured and their basic performance parameters were determined. It was found that the spectral characteristics of a quantum efficiency exhibit an increase for short wavelengths and this behavior has been linked with the plasmonic effect.

Key words: solar cells, ZnO, Si, heterojunction, nanorods, nanoparticles.

1. Introduction

Zinc oxide is intensively studied for the application in optoelectronics and photovoltaics due to a wide band gap (3.44 eV) and large exciton energy (60 meV) [1]. Undoped ZnO exhibits n-type conductivity that results from oxygen vacancies and zinc interstitials [2, 3], which in turn causes some difficulties in the fabrication of the p-type ZnO. However, it is an excellent candidate for heterostructures with p-type silicon [4, 5]. Among many methods of ZnO growth, atomic layer deposition seems to be the most attractive because of its simplicity and not very strict growth conditions – low pressure and temperature, which leads to reduction of production costs [6].

Zinc oxide nanorods can be attractive for photovoltaics due to the high surface-volume ratio. The easiest and most economical method of synthesizing ZnO nanorods is the hydrothermal method [7]. Coating the structures with metallic nanoparticles (silver, gold) leads to plasmonic effects, which not only affects the absorption and scattering, but also increases the efficiency of solar cells [8].

In this paper the structures based on p-type silicon and n-type zinc oxide nanorods covered with silver nanoparticles of two diameters, 20–30 nm and 50–60 nm, were studied for application in photovoltaics.

2. Preparation of the samples

Silicon wafers with the resistivity of 2 Ωcm and the thickness of 200 μm were used as a substrate. Pieces sized 1×1 cm were cleaned in 2-propanol, acetone and deionized water for 5 minutes in an ultrasonic washer. Then in ten cycles of the ALD process, ZnO nanoseeds were deposited, which initiated the growth of the ZnO nanorods using the hydrothermal method. The reaction solution consisted of zinc acetate dissolved in the deionized water. Adding sodium hydroxide to the solution changed pH to 7. The growth of the nanorods was performed under atmospheric pressure at 60°C.

Two samples were measured with different sizes of nanoparticles. On the top of the nanorods silver nanoparticles of 20–30 nm and 50–60 nm diameters were deposited using a short-time sputtering method. As a top transparent electrode, an AZO layer with a 3% Al content was used. Gold ohmic contacts were deposited at the bottom of the structure.

*e-mail: katarzyna.r.gwozdz@pwr.edu.pl

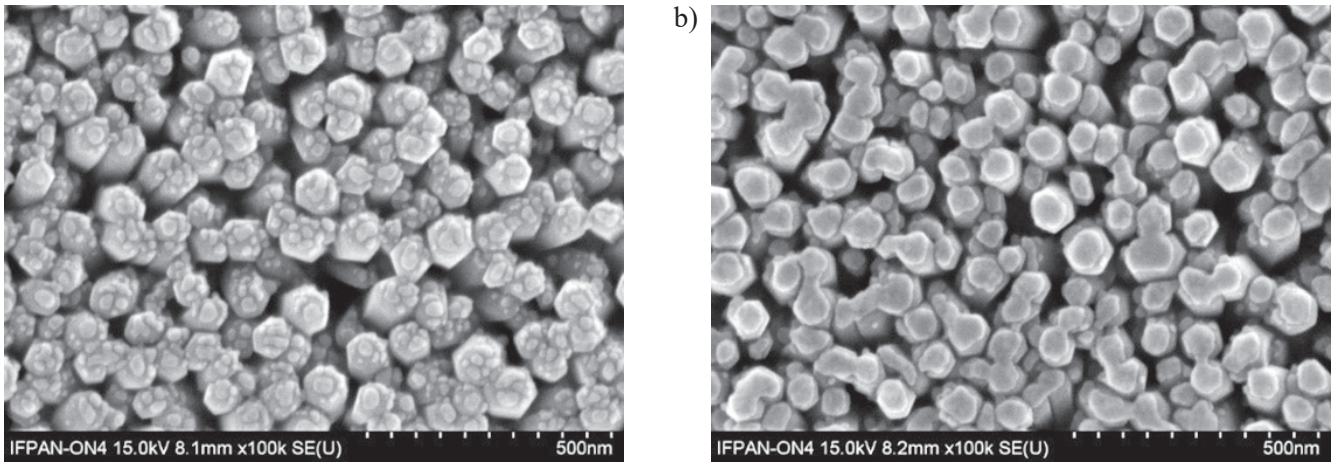

Fig. 1. SEM images for a) the sample with nanoparticles sized 20–30 nm, and b) the sample with nanoparticles sized 50–60 nm

3. Results and discussion

3.1. Scanning electron microscopy. SEM images before the deposition of the AZO layer for both samples are shown in Fig. 1. The nanorods have hexagonal shapes, which indicates a wurzite structure. The width of the nanorods is ~100 nm. The silver nanoparticles are clearly visible and their sizes are as expected. The density of the nanoparticles is 6×10^{14} m^{-2} for the smaller ones and 2×10^{14} m^{-2} for the bigger ones. The smaller nanoparticles are well separated, while the bigger ones exhibit the tendency to coalesce.

3.2. Atomic force microscopy. Fig. 2a shows the AFM image of the sample with nanoparticles sized 20–30 nm before the deposition of the AZO layer. In Fig. 2b the cross-section along the black line in Fig. 2a is shown. The density of the nanorods equals ~2×10^{13} m^{-2} for the sample with smaller nanoparticles and ~2.6×10^{13} m^{-2} for the sample with bigger nanoparticles. The nanorods have the width of ~100 nm, as it is seen in the SEM images. The divergence between the heights of the nanorods equals ~20 nm.

3.3. Raman spectroscopy and photoluminescence. Room temperature Raman and photoluminescence spectra were measured, under the excitation of the 514 nm argon laser, using a Jobin Yvon T64000 spectrometer and a CCD camera. The laser beam was focused on the area of around 1 μm by the lens with a ×100 magnification.

In Fig. 3a, which shows photoluminescence spectra, one can see only one peak around 375 nm caused by exciton annihilation [9]. This indicates the high quality of the nanorods.

Figure 3b presents Raman spectra of the samples before the deposition of the AZO layer. The peaks appearing around 303 cm^{-1} and 521 cm^{-1} are connected with the silicon substrate [10]. The other peaks are associated with the ZnO. Raman active modes for ZnO are A1(TO) = 380 cm^{-1}, A1(LO) = 574 cm^{-1}, E1(TO) = 407 cm^{-1}, E1(LO) = 583 cm^{-1}, E2(low) = 101 cm^{-1}, E2(high) = 437 cm^{-1} [11].

The presence of the peak E2(high) indicates the hexagonal structure of the nanorods. However, the peak is wider and shifted towards higher frequencies with comparison to the E2(high) mode of the bulk ZnO. This is due to the spatial phonon confinement [12].

The peak around 561 cm^{-1} is connected with the scattering on surface phonons, when the nanorods are smaller than the wavelength [13]. Surface phonon modes are found between the A1(LO) and E1(LO) modes [14]. The peak around 476 cm^{-1} can be assigned to the lower surface mode (LSM), while the peak around 561 cm^{-1} – to the upper surface mode (USM) [14]. The presence of these modes indicates the orientation of the nanorods along the c-axis, which was confirmed by the SEM images.

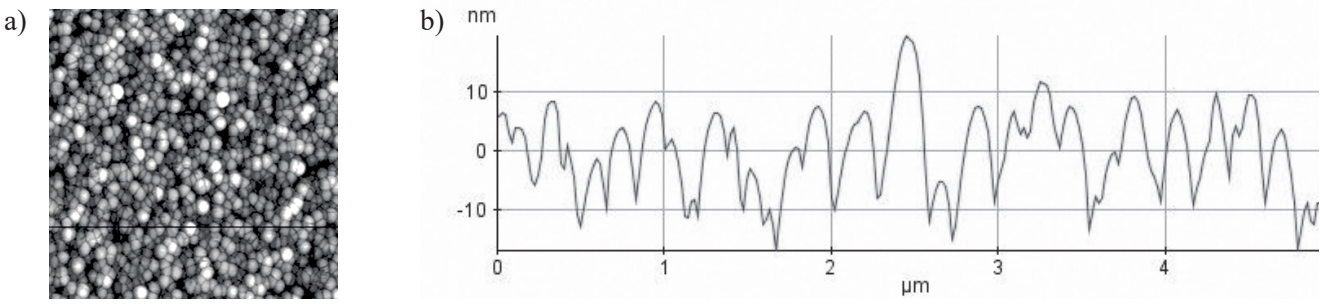

Fig. 2. a) An AFM image for the sample with the nanoparticles sized 20–30 nm in the 5×5 μm area, b) a cross-section along the black line marked in Fig. 2a

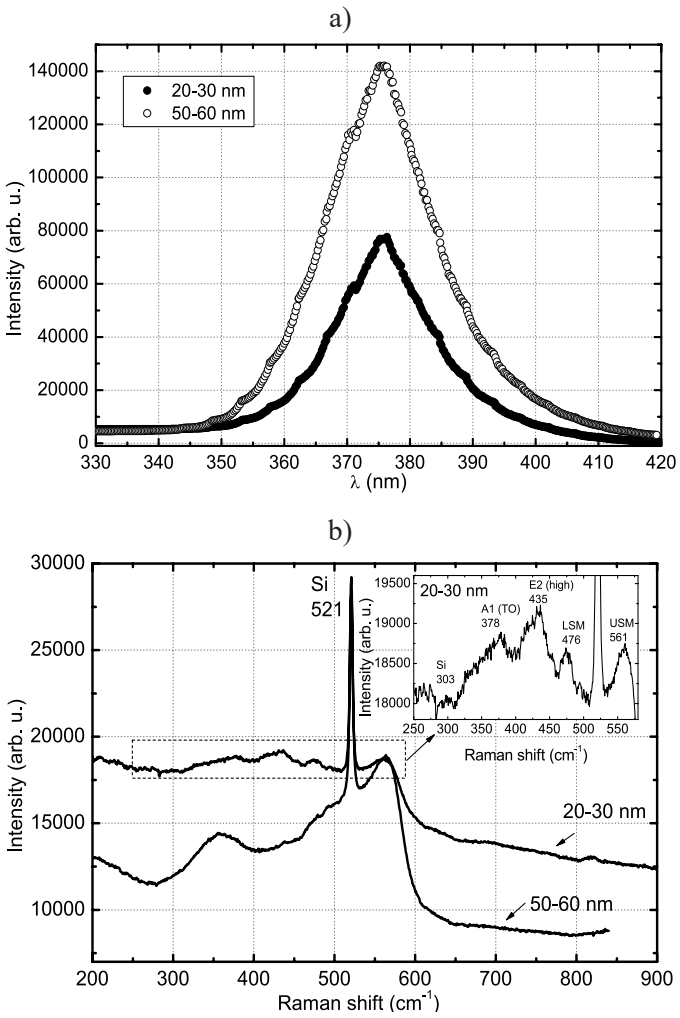

Fig. 3. a) Photoluminescence for the samples before the growth of the AZO layer, b) Raman spectra for the samples before the growth of the AZO layer. The inset shows the magnification of the Raman spectra for the sample with nanoparticles sized 20–30 nm. LSM and USM – surface modes

3.4. Current-voltage characteristics and quantum efficiency. The current-voltage characteristics were measured in the temperature of 25°C without illumination (Fig. 4a), with 1-sun illumination (Fig. 4b), and while changing the intensity of the illumination (Fig. 5).

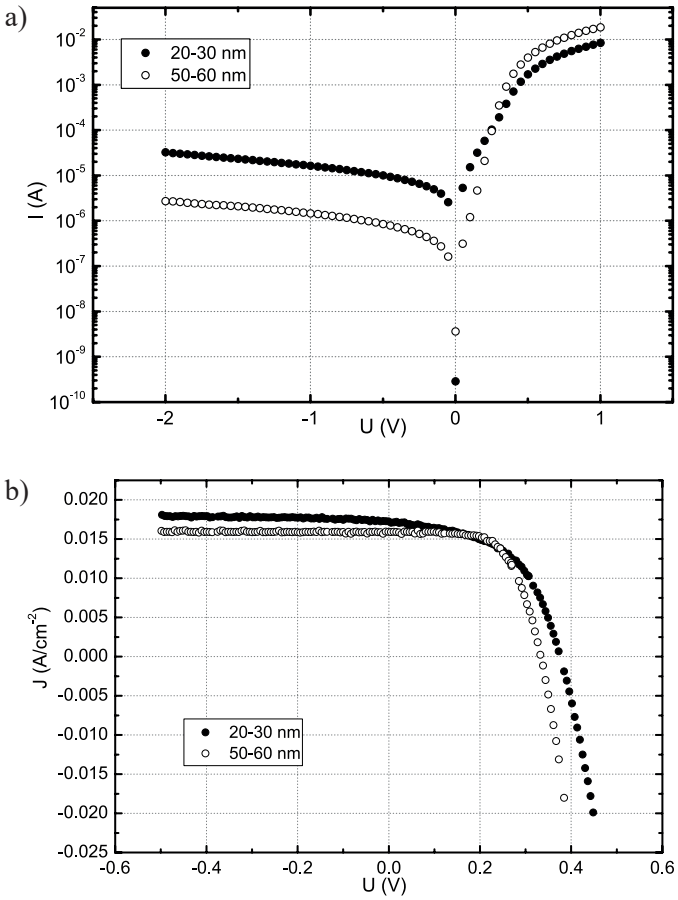

Fig. 4. a) I-V characteristics without illumination, b) J-V characteristics with 1-sun illumination (J – current density)

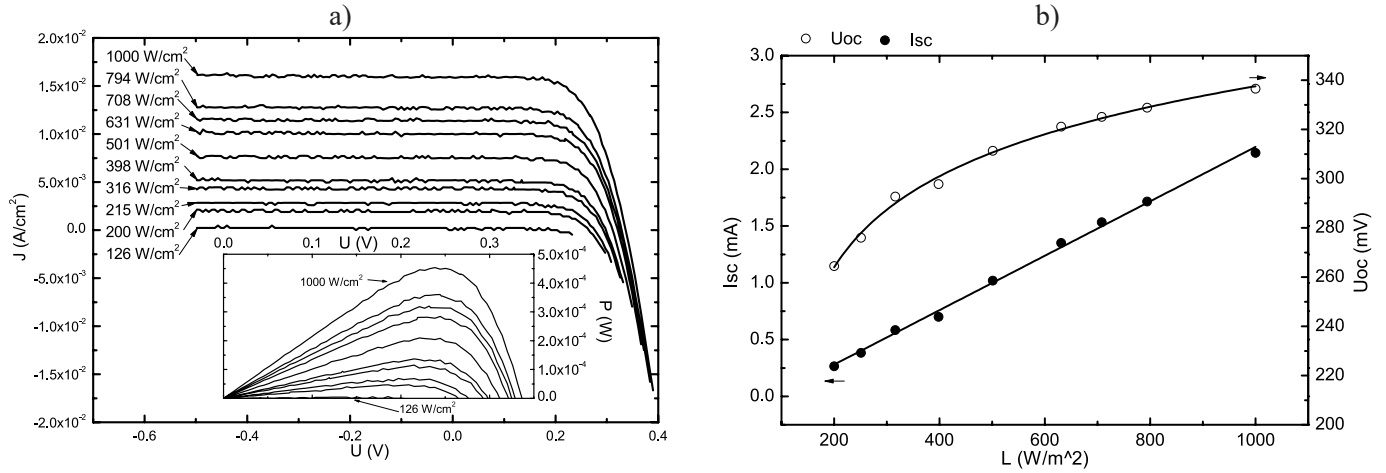

Fig. 5. a) The dependence between J-V characteristics and the intensity of the illumination, the inset shows the power generated for different intensities of the illumination b) the dependence between the short-circuit current, the open-circuit voltage, and the intensity of the illumination; solid lines mark theoretical calculations

Table 1
Parameters obtained from I-V characteristics; n – ideality factor, Rs – series resistance, V_{OC} – open-circuit voltage, J_{SC} – density of the short-circuit current, J_D – density of the diffusion current, J_R – density of the recombination current, P_m – maximum generated power, FF – fill factor, η – efficiency

Sample	n	R_s (Ω)	V_{OC} (V)	J_{SC} (mA/cm^2)	J_D (mA/cm^2)	J_R (mA/cm^2)	P_m (mW)	FF	η (%)
20–30 nm	2.35	58.73	0.376	17.25	2.2×10^{-11}	1.1×10^{-5}	0.62	0.53	3.4
50–60 nm	1.30	31.32	0.333	15.85	2.5×10^{-8}	8.5×10^{-6}	0.45	0.63	3.35

From Fig. 4a it can be concluded that the samples have good rectifying properties. The rectifying coefficient at ±1 V equals 632 for the samples with nanoparticles of the size of 20–30 nm and 1.3x10^4 for those sized 50–60 nm. Ideality factor n and series resistance R_s were determined from the dark I-V characteristics and collected in Tab. 1.

The other parameters shown in Table 1 were obtained from the light characteristics shown in Fig. 4b. Higher efficiency (3.4%) is exhibited by the sample with 20–30 nm nanoparticles, although the efficiencies differ only slightly – by 0.05 %. The low efficiency may be the result of the electrically active defects, such as recombination centers in the silicon, in the ZnO nanorods or at the interface between the silicon and the nanorods, which is implied by the fact that the recombination current density is much higher than the diffusion current density (see Table 1).

In Fig. 5a J-V characteristics (J – current density) and power versus illumination intensity, L, for the sample with the 50–60 nm nanoparticles are shown. The highest power is generated for the illumination intensity equal to 1000 W/m^2. Along with the decrease of the illumination intensity, the power decreases, too. Fig. 5b presents the relationship between the short-circuit current, the open-circuit voltage, and the illumination intensity. These dependencies are in agreement with theoretical assumptions that $I_{SC} \sim L$ and $U_{OC} \sim \ln(L)$. The sample with smaller nanoparticles exhibits the same relationships.

Usually the dependence of the short-circuit current vs the illumination intensity follows the relationship [15]:

$$I_{SC} = L^{\gamma} \tag{1}$$

The recombination coefficient, γ, can be obtained from the plot of the dependence in a logarithmic scale. If the recombination coefficient is greater than 1 or less than 0.5, the recombination at the surface dominates, whereas the recombination coefficient ranging between 0.5 and 1 is characteristic for a continuous distribution of trapping centers [15].

The dependence between the short-circuit current and the illumination intensity for the sample with the 50–60 nm nanoparticles is shown in Fig. 6a. The value of γ determined from this dependence equals 1.3 for the sample with bigger nanoparticles. The same value was obtained for the sample with smaller nanoparticles. Thus the recombination at the surface dominates in the studied solar cells and these results are in agreement with the results obtained from the light I-V characteristics, yielding much higher recombination in comparison to the diffusion current (see Table 1).

Fig. 6b presents the spectral dependence of external quantum efficiency, EQE, in the wavelength range of 300-1100 nm

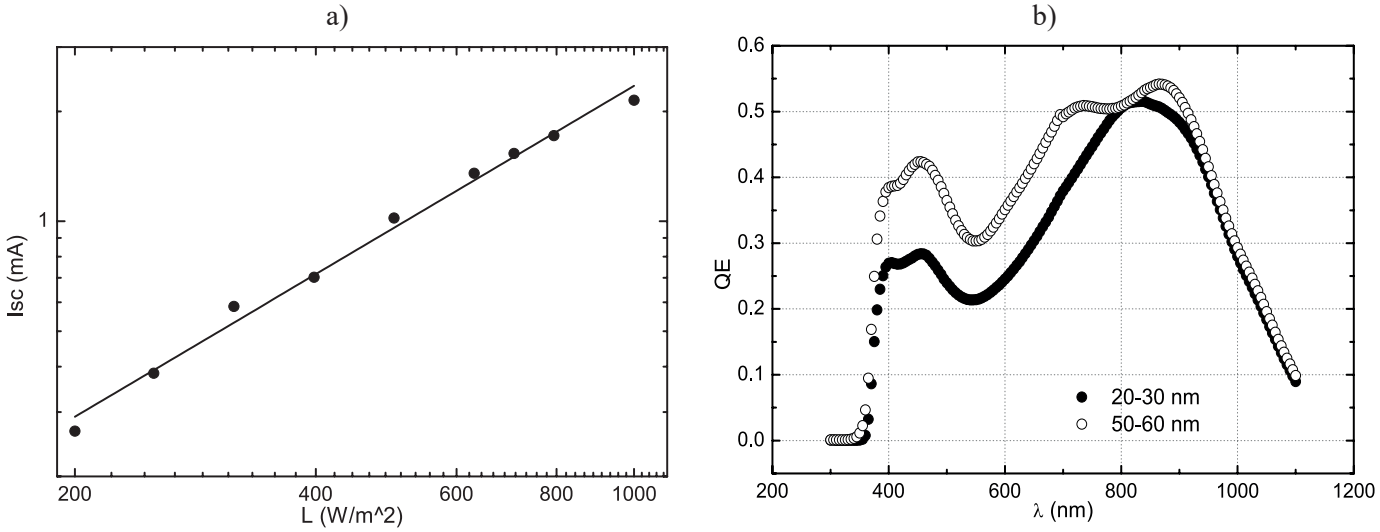

Fig. 6. a) The dependence between the short-circuit current and the intensity of the illumination in the logarithmic scale, b) external quantum efficiency spectrum

for both samples. The higher efficiency is observed for the sample with 50–60 nm nanoparticles and it is connected with the lower value of the series resistance of the sample (see Table 1). Both samples exhibit an increase of the EQE in the wavelength range of 400–500 nm. This increase cannot stem from the band-to-band transition in the ZnO layer, because its energy gap forbids the absorption in this wavelength range. However, the increase may be due to the near-band absorption in ZnO [16]. In our recent paper we have shown that the increase of EQE in this wavelength range is much smaller for a similar structure but without silver nanoparticles, and therefore we assigned this effect to the plasmonic effect in the ZnO nanorods [17]. According to the results presented in [18], the plasmonic effect has a range of approximately 1 μm. In the case of the studied structures, the nanorods have an average height of 1 μm [17]. Therefore it may be assumed that the plasmonic effect is not related to the Si substrate (which is also covered by the nanoparticles) because it is located too far from the surface. For the sample with bigger nanoparticles there is a local minimum at around 800 nm which may be a consequence of the local maximum appearing on its reflectivity spectrum at this wavelength [17].

4. Conclusions

In this paper, the structures based on p-type silicon and n-type zinc oxide nanorods covered with silver nanoparticles of sizes 20–30 nm and 50–60 nm in the context of their photovoltaic applications were investigated. Topography measurements with the use of AFM and SEM gave information about the sizes and density of the nanorods and the nanoparticles. The photoluminescence spectra confirmed the good quality of the structures. The SEM images as well as the Raman spectra allowed us to conclude that the nanorods have a hexagonal wurtzite structure. After the deposition of the AZO layer using the ALD method, the I-V characteristics were obtained, which allowed for determining the efficiency of the solar cells – 3.4% for the sample with the smaller nanoparticles. Simultaneously, the sample with bigger nanoparticles was shown to exhibit higher quantum efficiency in the wavelength range of 380–900 nm. That causes the difficulties in concluding which size of the nanoparticles is optimal for photovoltaics.

Acknowledgements. This work has been partially supported by the Polish-Taiwanese/Taiwanese-Polish Joint Research Project DKO/PL-TW1/3/2013 and by the project of the National Laboratory of Quantum Technologies (POIG. 02.02.00–00–003/08–00) and the National Science Centre (Decision Nos. DEC-2012/06/A/ST7/00398 and DEC-2013/11/B/ST7/01385).

References

[1] A. Janotti and C.G. Van de Walle, "Fundamentals of zinc oxide as a semiconductor", *Reports On Progress In Physics*, 72(12), 126501 (2009).

[2] F. Oba, M. Choi, A. Togo and I. Tanaka, "Point defects in ZnO: an approach from first principles", *Science And Technology Of Advanced Materials*, 12(3), 034302 (2011).

[3] A. Janotti and C.G. Van De Walle, "Native point defects in ZnO", *Physical Review B: Condensed Matter and Materials Physics*, 76(16), 165202 (2007).

[4] R. Pietruszka, G. Luka, K. Kopalko, E. Zielony, P. Bieganski, E. Placzek-Popko and M. Godlewski, "Photovoltaic and photoelectrical response of n-ZnO/p-Si heterostructures with ZnO films grown by an atomic layer deposition method", *Materials Science in Semiconductor Processing*, 25, 190–196 (2014).

[5] S. Sharma and C. Periasamy, "A study on the electrical characteristic of n-ZnO/p-Si heterojunction diode prepared by vacuum coating technique", *Superlattices and Microstructures*, 73, 12–21 (2014).

[6] E. Guziewicz, I.A. Kowalik, M. Godlewski, K. Kopalko, V. Osinniy, A. Wójcik, S. Yatsunenko, E. Łusakowska, W. Paszkowicz and M. Guziewicz, "Extremely low temperature growth of ZnO by atomic layer deposition", *Journal of Applied Physics*, 103, 033515 (2008).

[7] R. Pietruszka, B.S. Witkowski, G. Luka, L. Wachnicki, S. Gieraltowska, K. Kopalko, M. Godlewski, E. Zielony, P. Bieganski and E. Placzek-Popko, "Photovoltaic properties of ZnO nanorods/p-type Si heterojunction structures", *Beilstein Journal of Nanotechnology*, 5, 173–179 (2014).

[8] H.A. Atwater and A. Polman, "Plasmonics for improved photovoltaic devices", *Nature Materials*, 9, 205–213 (2010).

[9] K. Wu, Y. Lu, H. He, J. Huang, B. Zhao and Z. Ye, "Enhanced near band edge emission of ZnO via surface plasmon resonance of aluminum nanoparticles", *Journal of Applied Physics*, 110, 023510 (2011).

[10] J.H. Parker, D.W. Feldman and M. Ashkin, "Raman scattering by silicon and germanium", *Physical Review*, 155, 712–714 (1967).

[11] R. Cuscó, E. Alarcón-Lladó, J. Ibáñez, L. Artús, J. Jiménez, B. Wang and M.J. Callahan, "Temperature dependence of Raman scattering in ZnO", *Physical Review B: Condensed Matter and Materials Physics*, 75, 165202 (2007).

[12] S.M. Soosen, J. Koshy, A. Chandran and K.C. George, "Optical phonon confinement in ZnO nanorods and nanotubes", *Indian Journal of Pure and Applied Physics*, 48, 703–708 (2010).

[13] R. Ruppin, "Thermal fluctuations and Raman scattering in small spherical crystals", *Journal of Physics C: Solid State Physics*, 8, 1969–1978 (1975).

[14] B. Jusserand and M. Cardona, "Raman-spectroscopy of vibrations in superlattices", *Topics in Applied Physics*, 66, 49–152 (1989).

[15] I.S. Yahia, F. Yakuphanoglu, S. Chusnutdinow, T. Wojtowicz and G. Karczewski, "Photovoltaic characterization of n-CdTe/p-CdMnTe/GaAs diluted magnetic diode", *Current Applied Physics*, 13, 537–543 (2013).

[16] L.C. Chen and C.N. Pan, "Photoresponsivity enhancement of ZnO/Si photodiodes through use of an ultrathin oxide interlayer", *European Physical Journal: Applied Physics*, 44, 43–46 (2008).

[17] E. Placzek-Popko, K. Gwozdz, Z. Gumienny, E. Zielony, R. Pietruszka, B.S. Witkowski, Ł. Wachnicki, S. Gieraltowska, M. Godlewski, W. Jacak and L.-B. Chang, "Si/ZnO nanorods/Ag/AZO structures as promising photovoltaic plasmonic cells", *Journal of Applied Physics*, 117, 193101 (2015).

[18] W. Jacak, J. Krasnyj, J. Jacak, W. Donderowicz and L. Jacak, "Mechanism of plasmon-mediated enhancement of photovoltaic efficiency", *Journal of Physics D: Applied Physics*, 44, 055301 (2011).